Ultrasonics 96 (2019) 214–219

Contents lists available at ScienceDirect

Ultrasonics

journal homepage: www.elsevier.com/locate/ultras

A mathematical model of sonoporation using a liquid-crystalline shelled microbubble

James Cowley, Sean McGinty*

Division of Biomedical Engineering, University of Glasgow, Glasgow G12 8QQ, UK

ABSTRACT

In recent years there has been a great deal of interest in using thin shelled microbubbles as a transportation mechanism for localised drug delivery, particularly for the treatment of various types of cancer. The technique used for such site-specific drug delivery is sonoporation. Despite there being numerous experimental studies on sonoporation, the mathematical modelling of this technique has still not been extensively researched. Presently there exists a very small body of work that models both hemispherical and spherical shelled microbubbles sonoporating due to acoustic microstreaming. Acoustic microstreaming is believed to be the dominant mechanism for sonoporation via shelled microbubbles. Rather than considering the shell of the microbubble to be composed of a thin protein, which is typical in the literature, in this paper we consider the shell to be a liquid-crystalline material. Up until now there have been no studies reported in the literature pertaining to sonoporation of a liquid-crystalline shelled microbubble. A mathematical expression is derived for the maximum wall shear stress, illustrating its dependency on the shell's various material parameters. A sensitivity analysis is performed for the wall shear stress considering the shell's thickness; its local density; the elastic constant of the liquid-crystalline material; the interfacial surface tension and; the shell's viscoelastic properties. In some cases, our results indicate that a liquid-crystalline shelled microbubble may yield a maximum wall shear stress that is two orders of magnitude greater than the stress generated by commercial shelled microbubbles that are currently in use within the scientific community. In conclusion, our preliminary analysis suggests that using liquid-crystalline shelled microbubbles may significantly enhance the efficiency of site-specific drug delivery.

1. Introduction

Premanufactured shelled microbubbles are currently used in the UK as ultrasound imaging agents [1]. Recent research has focussed on using these shelled microbubbles as a transportation device for localised drug delivery in the treatment of various types of cancer [2–7]. However, despite significant research activity, this has not yet been achieved. The microbubbles, more commonly referred to as ultrasound contrast agents (UCAs), are typically composed of a layer or several layers of a thin protein shell encapsulating a perfluoro gas which stabilises the shelled microbubble when it is injected into the patient's bloodstream [8–10]. UCAs have a typical radius of between 1 μm and 4 μm, thus allowing them to migrate through the capillaries in the human body, and shell thicknesses of between 4 nm up to 100 nm depending on whether the UCA is a monolipid or polymer variant [11]. They typically resonate with frequencies in the range of 1–10 MHz producing nonlinear multiple harmonic signals that enhance the quality of the medical imaging process [12]. Rather than considering the shell of the microbubble to be composed of a thin protein, in this paper we consider the shell to be a liquid-crystalline material.

Liquid crystals are organic compounds that exhibit mesophase characteristics ([13], pp. 2). This means that they are intermediate states of matter lying between a solid and a liquid phase. They can be thought of as elongated rod-like molecules with a preferred local average direction. In this paper we use nematic liquid crystal theory ([13], pp. 133–159) to model the shell of the microbubble. Nematic liquid crystals possess both a viscous stress and a stress associated with the liquid crystal's elastic energy density. A nematic requires 5 independent viscosities to describe the liquid crystal's viscous stress ([13], pp. 151). It is the combinations of these Leslie viscosities that have physical significance ([13], pp. 155 & pp. 158). The elastic energy density of the nematic is described in terms of 3 elastic constants. These 3 independent elastic constants describe the splay, bend and twist contributions to the elastic energy density ([13], pp. 16). Since the stress of a liquid-crystalline shell is described in terms of a viscous stress rather than a stress associated with a stiffness (shear modulus), we speculate that the wall shear stress generated by a liquid-crystalline shelled microbubble may differ significantly from the stress associated with a commercial protein based shelled microbubble. We hypothesise that the unique physical properties of liquid crystals may make them a more suitable candidate for localised drug delivery than current protein shelled microbubbles.

The technique of sonoporation is one promising mechanism for site-specific drug delivery of UCAs. Sonoporation is the process of temporarily enhancing the porosity of the capillary walls using a combination of high frequency ultrasound signals in conjunction with shelled

* Corresponding author.
E-mail address: sean.mcginty@glasgow.ac.uk (S. McGinty).

https://doi.org/10.1016/j.ultras.2019.01.004
Received 3 August 2018; Received in revised form 17 January 2019; Accepted 17 January 2019
Available online 22 January 2019
0041-624X/

microbubbles [14]. This temporary enhancement of the capillary walls provides a potential "doorway" to the tumour. Despite the current volume of active experimental studies into sonoporation, the mechanisms causing sonoporation are still not fully understood. There are several possible processes for sonoporation via shelled microbubbles with acoustic microstreaming being one of the most common candidates. Doinikov and Bouakaz discuss in greater detail several other potential candidates for sonoporation via shelled microbubbles [14]. It is important to realise that sonoporation only occurs if the action on the capillary wall is highly localised. If we exclude the presence of shelled microbubbles then the cell will only undergo a uniform compression and expansion which is a global effect. It is worth noting that the shear stress that is exerted on the endothelial cells of the cellular wall as a consequence of blood flow is also a global effect. This is because the shear stress is applied across the whole surface of the capillary walls [15]. Using shelled microbubbles which are located very close to an irradiated cell results in the shelled microbubbles re-scattering the incident high frequency ultrasound waves which subsequently enhances the wall shear stress. Note that only a small region of the capillary wall, which must be in the close vicinity to the shelled microbubbles, will experience this highly localised wall shear stress.

The aim of this paper is to investigate how a liquid-crystalline shelled microbubble may enhance the wall shear stress exerted on a rigid plane compared to commercial protein shelled microbubbles.

The liquid-crystalline shelled microbubble is subjected to an external ultrasound pressure source that is pulsating at a frequency that is equal in magnitude to the liquid-crystalline shelled microbubble's natural frequency of oscillation. A sensitivity analysis is performed using the derived expression for the maximum wall shear stress and its dependency on the shell's material parameters is discussed in detail. The maximum wall shear stress generated by a typical liquid-crystalline shelled microbubble is compared to the stress generated by UCA's such as Sonovue which is currently under experimental investigation.

2. Theory of sonoporation

In 1958, Nyborg developed a mathematical model for acoustic microstreaming [16]. Acoustic microstreaming is the induced vortical flow experienced by a small object such as a shelled microbubble when it is in close locality to a fluid-solid interface whilst being subjected to a high frequency sinusoidal external acoustic pressure signal. Nyborg's model allows us to evaluate the wall shear stress induced on a rigid plane wall due to acoustic microstreaming as a direct consequence of a re-scattering shelled microbubble which is in close proximity to the rigid plane boundary wall. However, note that the model developed by Nyborg is only applicable to a pulsating hemispherical shelled microbubble. Rooney proposed that the wall shear stress, denoted by τ, could be expressed in terms of the displacement amplitude of the shelled microbubble which is denoted by η_m [17]. The resulting wall shear stress is given by

$$\tau = 2(\rho_L \mu_L)^{1/2}(\pi f)^{3/2}\eta_m^2/R_0, \tag{1}$$

where ρ_L is the density of the liquid medium surrounding the pulsating shelled microbubble, μ_L is the viscosity of this liquid medium, f is the driving frequency of the ultrasound signal and R_0 is the equilibrium radius of the shelled microbubble. Levin and Bjørnø hypothesised that the Rayleigh-Plesset equation could be used to evaluate η_m [18]. Doinikov and Bouakaz extended Nyborg's model further by considering the scenario of a spherical shelled microbubble rather than Nyborg's hemispherical model [14]. The model that they developed only considered a pulsating shelled microbubble in the xz plane with boundary conditions that were valid for a plane boundary that was rigid and inelastic in behaviour. Glaser estimated the rigidity of the membrane of lymphocytes to have an elastic modulus of 80 MPa ([19], pp. 87–91). This relatively high value indicates that a cell and consequently the capillary wall can be assumed to be rigid and inelastic in nature. The additional boundary conditions required due to the rigid plane wall for the specific type of Rayleigh-Plesset model are derived and discussed in detail in several journal articles [20–22].

2.1. Model for the liquid-crystalline shelled microbubble

For the purposes of this feasibility study, we view the liquid–crystal as being of the nematic type, and there are five associated Leslie viscosity coefficients. For further details the reader is referred to ([13], pp. 151). We utilise a Rayleigh-Plesset model developed by Cowley which considers the shell as a liquid-crystalline material and makes use of a simplified strain energy density function [23]. Refer to Appendix A for a summarised derivation of the liquid-crystalline shelled microbubble model. We briefly describe the model here, but refer the reader to [23] for full details. This model accounts for the thickness of the shell and considers both the shell's interfacial surface tension (internal gas-shell interface) and the surface tension on the exterior of the shell due to the action of the surrounding fluid (shell-fluid interface). Cowley proposes that the radial motion of a liquid-crystalline shelled microbubble near a rigid plane wall can be described by

$$\begin{aligned} R_1\ddot{R}_1\left(1-\left(\frac{\rho_S-\rho_L}{\rho_S}\right)\frac{R_1}{R_2}\right)+\dot{R}_1{}^2\left(\frac{3}{2}-\left(\frac{\rho_S-\rho_L}{\rho_S}\right)\left(\frac{4R_1R_2^3-R_1^4}{2R_2^4}\right)\right) \\ =\frac{1}{\rho_S}\left(\left(P_0+\frac{2\sigma_1}{R_{01}}+\frac{2\sigma_2}{R_{02}}+4K_1\left(\frac{1}{R_{01}^2}-\frac{1}{R_{02}^2}\right)\right)\left(\frac{R_{01}}{R_1}\right)^{3\kappa}-\frac{2\sigma_1}{R_1}-\frac{2\sigma_2}{R_2}\right. \\ \left.-P_0-P_{acoustic}(t)\right)-\frac{1}{\rho_S}\left(\alpha\left(\frac{\dot{R}_1}{R_1}-\frac{\dot{R}_2}{R_2}\right)+4K_1\left(\frac{1}{R_1^2}-\frac{1}{R_2^2}\right)+\frac{4\mu_L\dot{R}_2}{R_2}\right) \\ -(R_2\ddot{R}_2+2\dot{R}_2{}^2)\frac{R_2}{2d}, \end{aligned} \tag{2}$$

where $R_1(t)$ and $R_2(t)$ are the instantaneous inner and outer radius of the microbubble respectively, $\dot{R}_1$ and $\dot{R}_2$ denote the speed of the inner and outer radius of the microbubble, $\ddot{R}_1$ and $\ddot{R}_2$ are the acceleration of the inner and outer radius of the microbubble, whilst R_{01} and R_{02} denote the inner and outer equilibrium radius. The hydrostatic pressure in the surrounding Newtonian fluid is represented by P_0;σ_1 is the surface tension between the gas-shell interface; σ_2 is the surface tension at the shell-fluid interface; the density of the shell is denoted by ρ_S and; the density of the surrounding liquid is given by ρ_L. The term α represents a combination of the nematic Leslie viscosities of the liquid-crystalline shell, which is unique to the specific type of liquid–crystal, and is given by [23].

Fig. 1 illustrates the shelled microbubble pulsating in close vicinity to the rigid plane wall. Other physical parameters include the ratio of specific heats of the gas within the microbubble (κ); the driving acoustic pressure ($P_{acoustic}(t)$); the elastic constant which is a unique material property of the liquid-crystalline shell (K_1); the viscosity of the surrounding Newtonian fluid (μ_L) and; the distance between the centre of the microbubble and the capillary wall (d), which is assumed to be a rigid plane wall. The boundary conditions for the rigid plane results in

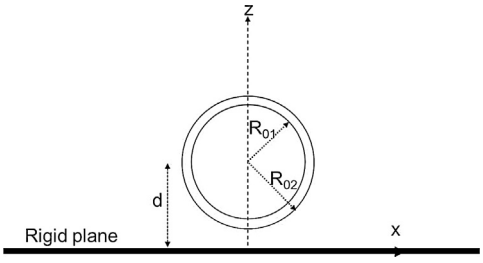

Fig. 1. A shelled microbubble of inner radius R_{01} and outer radius R_{02} pulsating in the locality of a rigid plane wall. The centre of the microbubble is at a distance d from the rigid wall.

the term given by

$$-(R_2\ddot{R}_2 + 2\dot{R}_2{}^2)\frac{R_2}{2d}. \tag{3}$$

The derivation of Eq. (3) is given in detail in several journal articles [20–22].

We assume that the surrounding fluid is Newtonian in behaviour [24–27] and that the shell is incompressible in nature ([13], pp. 139). The dynamics of a liquid-crystalline shelled microbubble given by Eq. (2) assumes that the shell is incompressible and that the surrounding fluid is Newtonian. We model this surrounding Newtonian fluid as an incompressible liquid, thus there are no acoustic radiation losses of the shelled microbubble due to a lack of compressibility of the surrounding fluid. Note that Doinikov and Bouakaz [14] assume that the surrounding fluid is compressible in nature resulting in an additional term in their Rayleigh-Plesset equation. This term is dependent on the speed of sound in the surrounding fluid as well as the radius of the outer shell, the velocity of the outer shell of the microbubble and its acceleration.

2.2. Further details on sonoporation

Doinikov and Bouakaz [14] refined Nyborg's theory to consider a spherical shelled microbubble that was detached from the plane. They modelled the irrotational liquid velocity generated by acoustic microstreaming subject to the boundary conditions detailed in the following articles [20–22]. Doinikov and Bouakaz adopted Nyborg's approach of linearisation. Linearising their expression for the irrotational liquid velocity by assuming that the outer radius experienced a small time dependent perturbation where $\dot{R}_2 = i\omega\eta_m\exp(i\omega t)$ and ω is the angular frequency of the ultrasound source, they obtained the following expression for the wall shear stress in the xz plane

$$\tau_{xz} = 2(\rho_L\mu_L)^{1/2}(\pi f)^{3/2}\frac{\eta_m^2}{R_{02}}\left(\frac{R_{02}}{d}\right)^5 F(\beta), \tag{4}$$

with $\beta = x/d$, where x is the distance in the x-plane. The β-dependent term in Eq. (4) is denoted by

$$F(\beta) = \frac{2\beta(1-2\beta^2)}{(1+\beta^2)^4}, \tag{5}$$

and has a maximum value of

$$\beta_{max} = \sqrt{\frac{13-\sqrt{129}}{20}}. \tag{6}$$

Eq. (4) shows that the wall shear stress increases with a decreasing d, yielding a maximum wall shear stress when $d = R_{02}$ which is when the shelled microbubble is in direct contact with the rigid plane wall. This suggests that the microbubble should be in the direct vicinity of the cellular wall in order for sonoporation to occur as efficiently as possible.

3. Linearisation of the model

Assuming that the amplitude of the microbubble oscillation is small [24–27], then we can say that inner radius $R_1(t)$ is given by

$$R_1 = R_{01} + \xi(t), \quad \text{where } |\xi(t)| \ll R_{01}, \tag{7}$$

and that the outer radius R_2 can be described as

$$R_2 = R_{02} + \eta(t), \quad \text{where } |\eta(t)| \ll R_{02}. \tag{8}$$

We assume, in line with other models [24–27], that the liquid-crystalline shell is incompressible and that there is no change in the local density of the shell. Using the formula for the volume of a sphere and applying the assumption that the shell is incompressible, then it follows that

$$R_2^3 - R_1^3 = R_{02}^3 - R_{01}^3 \Rightarrow (R_{02}+\eta(t))^3 - (R_{01}+\xi(t))^3 = R_{02}^3 - R_{01}^3. \tag{9}$$

Linearising Eq. (9) using Eqs. (7) and (8) results in

$$\eta(t) \approx \left(\frac{R_{01}}{R_{02}}\right)^2 \xi(t). \tag{10}$$

Linearising Eq. (2) using Eqs. (7), (8) and (10) yields

$$\ddot{\xi} + \gamma_d\dot{\xi} + \omega_0^2\xi = -\frac{P_{acoustic}(t)}{\rho_S\left(R_{01}\left(1-\left(\frac{\rho_S-\rho_L}{\rho_S}\right)\frac{R_{01}}{R_{02}}\right) + \frac{R_{01}^2}{2d}\right)}, \tag{11}$$

where the damping term γ_d, is given by

$$\gamma_d = \frac{\alpha\left(1-\left(\frac{R_{01}}{R_{02}}\right)^3\right) + 4\mu_L\left(\frac{R_{01}}{R_{02}}\right)^3}{\rho_S\left(R_{01}^2\left(1-\left(\frac{\rho_S-\rho_L}{\rho_S}\right)\frac{R_{01}}{R_{02}}\right) + \frac{R_{01}^3}{2d}\right)}, \tag{12}$$

which is related to the relaxation time by $t_{relax} = 1/\gamma_d$ (where the relaxation time is defined as the time taken for the amplitude to equal $1/e$ of its maximum value). The natural angular frequency is given by

$$\omega_0 = \sqrt{\frac{\mathrm{N}}{\mathrm{D}}}, \tag{13}$$

where

$$\mathrm{N} = 3\kappa R_{01}R_{02}^5(P_0 + 2\sigma_1/R_{01} + 2\sigma_2/R_{02}) - 2\sigma_1R_{02}^5 - 2\sigma_2R_{01}^4R_{o2} + (12\kappa - 8)K_1R_{02}^5/R_{01} + 8K_1R_{01}^4 - 12\kappa K_1R_{02}^3R_{01}, \tag{14}$$

and

$$\mathrm{D} = \rho_S\left(R_{01}^3R_{02}^5\left(1-\left(\frac{\rho_S-\rho_L}{\rho_S}\right)\frac{R_{01}}{R_{02}}\right) + \frac{R_{01}^4R_{02}^5}{2d}\right). \tag{15}$$

We can re-express the acoustic pressure ($P_{acoustic}(t)$) in terms of a complex exponential of the form $P_A\exp(i\omega t)$, where P_A is the maximum amplitude of the ultrasound pressure and ω is the driving angular frequency of the system. Assuming that the displacement can be written as $\xi(t) = \xi_m\exp(i\omega t - \phi)$, as discussed by [24–27], where ξ_m is the displacement amplitude and ϕ is the phase of the driving system, one finds on solving Eq. (11) that ξ_m is given by

$$\xi_m = \frac{P_A}{\rho_S\left(R_{01}\left(1-\left(\frac{\rho_S-\rho_L}{\rho_S}\right)\frac{R_{01}}{R_{02}}\right) + \frac{R_{01}^2}{2d}\right)\sqrt{(\omega_0^2-\omega^2)^2 + \omega^2\gamma_d^2}}. \tag{16}$$

Using Eq. (10) alongside Eq. (16), and substituting into Eq. (4) gives

$$\tau_{xz} = \left(\frac{\rho_L\mu_L}{2}\right)^{1/2}\left(\frac{\omega}{\omega_0}\right)^{3/2}\left(\frac{R_{01}^4}{d^5}\right)F(\beta) \times \frac{P_A^2}{\rho_S^2\left(R_{01}\left(1-\left(\frac{\rho_S-\rho_L}{\rho_S}\right)\frac{R_{01}}{R_{02}}\right) + \frac{R_{01}^2}{2d}\right)^2\omega_0^{5/2}\left(\left(1-\frac{\omega^2}{\omega_0^2}\right)^2 + \frac{\omega^2\gamma_d^2}{\omega_0^4}\right)}. \tag{17}$$

Eq. (17) highlights how the wall shear stress is a function of the distance d as well as the driving angular frequency ω. The maximum wall shear stress occurs when $d = R_{02}$, that is when the microbubble is in direct contact with the rigid wall, and when $\beta = \beta_{max}$. Using Eq. (5), we find that $F(\beta_{max}) \approx 0.349$. Note that the natural angular frequency ω_0 and the damping term γ_d are functions of d and are modified to ω_{0*} and γ_{d*} respectively for the microbubble when it is in direct contact with the rigid plane wall. The wall shear stress given by Eq. (17) has a dependency on the driving angular frequency and has a maximum value at the resonant frequency of the shelled microbubble [14].

We shall consider the wall shear stress when the microbubble is in immediate contact with the rigid plane wall, that is, when $d = R_{02}$ and at the driving angular frequency ω_{0*} which is the natural angular frequency of the system for $d = R_{02}$. The resulting expression for the wall shear stress is given by

$$\tau_{max}(\omega = \omega_{0*}) = \left(\frac{\rho_L \mu_L}{2}\right)^{1/2}\left(\frac{0.349}{R_{02}}\right)\left(\frac{R_{01}}{R_{02}}\right)^4 \left(\frac{P_A^2}{\rho_S^2\left(R_{01}\left(1-\left(\frac{\rho_S-\rho_L}{\rho_S}\right)\frac{R_{01}}{R_{02}}\right)+\frac{R_{01}^2}{2R_{02}}\right)^2 \omega_{0*}^{1/2}\gamma_{d*}^2}\right), \tag{18}$$

with

$$\gamma_{d*} = \frac{\alpha\left(1-\left(\frac{R_{01}}{R_{02}}\right)^3\right)+4\mu_L\left(\frac{R_{01}}{R_{02}}\right)^3}{\rho_S\left(R_{01}^2\left(1-\left(\frac{\rho_S-\rho_L}{\rho_S}\right)\frac{R_{01}}{R_{02}}\right)+\frac{R_{01}^3}{2R_{02}}\right)}, \tag{19}$$

and

$$\omega_{0*} = \sqrt{\frac{\mathrm{N}}{\mathrm{D}^*}}. \tag{20}$$

Hence D is altered for $d = R_{02}$ and is denoted by D^* which is given by

$$\mathrm{D}^* = \rho_S\left(R_{01}^3 R_{02}^5\left(1-\left(\frac{\rho_S-\rho_L}{\rho_S}\right)\frac{R_{01}}{R_{02}}\right)+\frac{R_{01}^4 R_{02}^4}{2}\right). \tag{21}$$

Note that accounting for the compressible nature of the surrounding fluid which Doinikov and Bouakaz [14] have done will not alter the linearised expression for the wall shear stress given by Eq. (18). Their article discusses this compressible term which contains both higher order terms and also first order terms which are expressed as a fraction of the speed of sound within the fluid. We can neglect the terms associated with a compressible fluid because the higher order terms are removed due to linearisation whilst the remaining first order terms, one of which is the shelled microbubble's velocity, are much smaller in magnitude than the speed of sound in the surrounding fluid.

4. Results and discussion

We shall now consider how the maximum wall shear stress given by Eq. (18) depends on various material parameters when the shelled microbubble is subjected to a typical sinusoidal ultrasound signal of pressure $P_A = 30$ kPa [14] and an angular frequency that is equal to the natural angular frequency ω_{0*} given by Eq. (20) via Eqs. (14) and (21). The material parameters such as the density of the shell and the liquid crystal's viscoelastic characteristics, are changed by varying the particular type of liquid crystal material. Different types of liquid crystals have very specific and unique material properties. Table 1 gives the material parameters used in the sensitivity analysis.

The linearisation is valid when the perturbed amplitude of the microbubble is significantly lower than the microbubble's equilibrium radius. This condition is valid provided that the externally applied ultrasound pressure load is small i.e. around 30 kPa. The perturbed amplitude is independent of the material parameters of the shell and surrounding fluid and is solely dependent on the externally applied ultrasound signal. The sensitivity analysis, which is dependent purely on the material parameters of the shell and the surrounding fluid, will hold for both the linear and non-linear equations. The sensitivity analysis performed for α, ρ_S and σ_1 is analagous to varying the types of nematic liquid crystals that are being used to make the microbubble's shell. Different nematic liquid crystals have different α, ρ_S and σ_1 values ([13], pp. 330). With the sensitivity analysis, we are attempting to identify the most suitable material parameters that are required to maximise the wall shear stress. We can see from Fig. 2(a) how the maximum wall shear stress τ_{max} increases approximately linearly with an increasing shell density ρ_S. We consider a small range of ρ_S values since this represents the typical spectrum of density values for liquid crystals, whose density is slightly larger than the density of water at standard room temperature. This approximately linear behaviour is valid over the typical range of values of ρ_S for liquid crystals. This is a consequence of the shell's increasing inertia since the shelled microbubble is in direct contact with the capillary wall. Analysis of Fig. 2(b) highlights how the maximum wall shear stress τ_{max} decreases nonlinearly as the Leslie viscosity contribution α increases. This is due to an increase in the damping term γ_{d*} given by Eq. (19) whose square varies inversely with the maximum wall shear stress τ_{max} as given by Eq. (18). Studying Fig. 2(c) illustrates how the maximum wall shear stress τ_{max} decreases nonlinearly as the surface tension at the gas-shell interface denoted by σ_1 increases. This is because an increase in the interfacial surface tension σ_1 changes the natural angular frequency ω_{0*} as we can see from Eqs. (14) and (20). An increase in σ_1 results in a larger natural angular frequency ω_{0*} which yields a smaller maximum wall shear stress τ_{max} which is given by Eq. (18). Observing Fig. 2(d) shows how the maximum wall shear stress τ_{max} decreases nonlinearly as the thickness of the shell increases from 4 nm to 100 nm. An increase in the thickness of the shell $R_{02} - R_{01}$ results in a larger damping term γ_{d*} as can be seen from Eq. (19). Referring to Eq. (18) we see that the maximum wall shear stress τ_{max} induced by the shelled microbubble is inversely proportional to the square of γ_{d*} which results in a nonlinear reduction in τ_{max}. Careful analysis of Eq. (18) reveals that the wall shear stress τ_{max} experiences very little change as the elastic constant varies over several orders of magnitude despite the natural angular frequency ω_{0*} displaying a dependency on K_1. The reason for this negligible variation in τ_{max} lies in the very small magnitude of K_1.

Table 1
Fixed material parameters [14].

Physical symbol	Value(s) (units)
μ_L	10^{-3} Pa s
ρ_L	1000 kg m^{-3}
κ	1.07
σ_2	0.072 N m^{-1}
R_{01}	0.996 μm

4.1. Comparing a liquid-crystalline shelled microbubble to a viscoelastic commercial contrast agent

We can compare and contrast the wall shear stress induced by a liquid-crystalline shelled microbubble developed in this paper (see Eq. (18)) with typical commercial contrast agents which are discussed in the paper by Doinikov and Bouakaz [14]. Commercial contrast agents such as Sonovue are modelled using a shear modulus which characteristically describes the shell's solid phase, and a viscoelastic contribution that is proposed to be either a Maxwell fluid or possibly Kelvin-Voigt in nature [24–27]. We can compare the wall shear stress given by Eq. (18) with Doinikov and Bouakaz's model. In order for the comparison to be fair, we shall use the same size of external ultrasound pressure, the same surrounding liquid viscosity and surface tension for the shell-liquid interface as well as the same liquid density and shell radius. We find that a liquid-crystalline shell of typical radius of the order of 1 μm [25], possessing a Leslie viscosity value of $\alpha = 0.03$ Pa s ([13], pp. 330) in conjunction with [23], and interfacial surface tension $\sigma_1 = 0.03$ N m^{-1} ([13], pp. 330) yields a wall shear stress $\tau_{max} \approx 2670$Pa for a typical ultrasonic pressure of magnitude $P_A = 30$ kPa compared to Doinikov and Bouakaz's value of $\tau_{max} \approx 15$ Pa [14].

This highlights that liquid-crystalline shelled microbubbles may enhance the wall shear stress significantly, by two orders of magnitude more than current, commercial contrast agents. Our analysis suggests that liquid-crystalline shelled microbubbles with material parameters described in ([13], pp. 330), which are typical of a nematic liquid crystal, may be more efficient at sonoporating than the current, licensed ultrasound contrast agents.

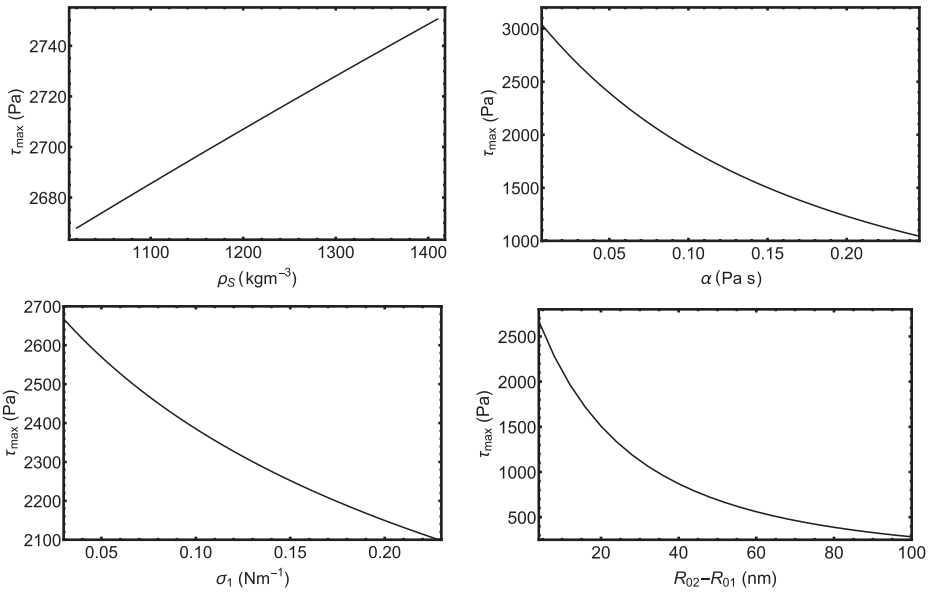

Fig. 2. A sensitivity analysis of the maximum wall shear stress (τ_{max}) generated by a shelled microbubble versus; **(a)** the density (ρ_S) of the liquid-crystalline shell; **(b)** the Leslie viscosity (α) of the liquid-crystalline shell; **(c)** the surface tension at the gas-shell interface (σ_1); **(d)** the thickness of the liquid-crystalline shell ($R_{02} - R_{01}$). Graphs (a)-(d) are constructed using Eqs. (14), (18)–(21) and Tables 1 and 2.

5. Conclusion

In this paper, we have developed a model for sonoporation via a liquid–crystal shelled microbubble which is in direct contact with a rigid plane wall. We performed a sensitivity analysis to identify the relationship between the wall shear stress and various material properties of the shell. Note that the linearisation is only valid provided $|\xi(t)| \ll R_{01}$ and $|\eta(t)| \ll R_{02}$. Our study highlights that the maximum wall shear stress decreases nonlinearly as the shell's surface tension (gas-shell interface) increases, as the shell's Leslie viscosity increases and as the shell's thickness increases. The maximum wall shear stress increases in an approximately linear manner as the shell's local density increases. We note that the elastic constant for the liquid-crystalline shell has a negligible effect on the wall shear stress. This sensitivity analysis may help both soft matter physicists and/or bioengineers identify the most suitable liquid-crystalline materials required to optimise sonoporation via shelled microbubbles. Our analysis suggests, in some cases, that liquid-crystalline shelled microbubbles may enhance the wall shear stress by two orders of magnitude more than current commercial contrast agents that are presently under investigation and may therefore be more efficient at sonoporating than the current, licensed ultrasound contrast agents. In principle, it is possible to identify the optimal material parameters required to give the desired wall shear stress that will induce sonoporation. At present there is no experimental data pertaining to sonoporation in capillary walls. We hope that this paper inspires future experimental work. We accept that further investigation is required both theoretically and experimentally to support our findings.

We wish to acknowledge that we have made a number of assumptions in this work. Now that we have demonstrated that liquid crystals have potential, we will look to relax these assumptions in future work. Future work should derive the Rayleigh-Plesset equation making use of a more accurate strain energy density function that fully accounts for the splay, twist and bend terms ([13], pp. 151) that are characteristic of nematics. Other future work will focus on modifying the wall to account for viscoelasticity. Our current study has modelled the surrounding fluid as a Newtonian fluid rather than a non-Newtonian fluid despite the fact that blood and blood plasma are known to be non-Newtonian in nature. We have modelled the shelled microbubble in two dimensions whereas a more sophisticated approach would be to consider not only all three dimensions but also non-spherical behaviour of the shelled microbubble. Doinikov and Bouakaz [14] have highlighted how the exposure time of the shelled microbubbles to an external ultrasound pressure influences the efficiency of sonoporation with greater exposure times resulting in more effective sonoporation. We have not considered exposure time in this study nor have we considered multiple microbubbles or indeed solutions of shelled microbubbles. Future work should consider the efficiency of a solution of liquid-crystalline shelled microbubbles sonoporating against a rigid wall when subjected to an external ultrasound pressure signal. We accept that experimental work is required to validate the speculations of the mathematical model.

Acknowledgements

The authors gratefully acknowledge the support given by the Carnegie Trust for the Universities of Scotland [Grant RIG007543].

Appendix A. Supplementary material

Some brief details of the derivation of the model for the liquid-

Table 2
Adjustable material parameters for sensitivity analysis [13], pp. 330.

Case	ρ_S (kg m^{-3})	α (Pa s)	σ_1 (N m^{-1})	$R_{02} - R_{01}$ (nm)	K_1 (pN)
a	1020 ↔ 1410	0.03	0.03	4	6
b	1020	0.0072 ↔ 0.246	0.03	4	6
c	1020	0.03	0.03 ↔ 0.228	4	6
d	1020	0.03	0.03	4 ↔ 100	6
e	1020	0.03	0.03	4	6 ↔ 600

crystalline shelled microbubble (2) are provided as supplementary material. Supplementary data associated with this article can be found, in the online version, at https://doi.org/10.1016/j.ultras.2019.01.004.

References

[1] P. Narayan, M.A. Wheatley, Preparation and characterization of hollow microcapsules for use as ultrasound contrast agents, Polym. Eng. Sci. 39 (1999) 2242–2255.

[2] M.B. Peregrino, B. Rifai, R.C. Carlisle, J. Choi, C.D. Arvanitis, L.W. Seymour, C.C. Coussios, Cavitation-enhanced delivery of a replicating oncolytic adenovirus to tumors using focused ultrasound, J. Controlled Release 169 (2013) 40–47.

[3] D. Gourevich, A. Volovick, O. Dogadkin, L. Wang, H. Mulvana, Y. Medan, A. Melzer, S. Cochran, In vitro investigation of the individual contributions of ultrasound-induced stable and inertial cavitation in targeted drug delivery, Ultrasound Med. Biol. 41 (2015) 1853–1864.

[4] J.M. Escoffre, C. Mannaris, B. Geers, A. Novell, I. Lentacker, M. Averkion, A. Bouakaz, Doxirubicin liposome-loaded microbubbles for contrast imaging and ultrasound triggered drug delivery, IEEE Trans. Ultrason., Ferroelectr. Freq. Control 60 (2013) 78–87.

[5] C.H. Fan, C.Y. Ting, H.L. Liu, C.Y. Huang, H.Y. Hsieh, T.C. Yen, K.C. Wei, C.K. Yeh, Antiangiogenic-targeting drug-loaded microbubbles combined with focused ultrasound for glioma treatment, Biomaterials 34 (2013) 2142–2155.

[6] F. Yan, L. Li, Z. Deng, Q. Jin, J. Chen, W. Yang, C.K. Yeh, J. Wu, R. Shandas, X. Liu, H. Zheng, Paclitaxel-liposome-microbubble complexes as ultrasound-triggered therapeutic drug delivery carriers, J. Controlled Release 166 (2013) 246–255.

[7] C. Niu, Z. Wang, G. Lu, T.M. Krupka, Y. Sun, Y. You, W. Song, H. Ran, P. Li, Y. Zheng, Doxorubicin loaded superparamagnetic PLGA-iron oxide multifunctional microbubbles for dual-mode US/MR imaging and therapy of metastasis in lymph nodes, Biomaterials 34 (2013) 2307–2317.

[8] E. Stride, N. Saffari, Microbubble ultrasound contrast agents: a review, Proc. Inst. Mech. Eng. Part H 217 (2003) 429–447.

[9] D. Cosgrove, Ultrasound contrast agents: an overview, Eur. J. Radiol. 60 (2006) 324–330.

[10] E. Stride, C.C. Coussios, Cavitation and contrast: the use of bubbles in ultrasound imaging and therapy, Proc. Inst. Mech. Eng. Part H 224 (2010) 171–191.

[11] J. McLaughlan, N. Ingram, P.R. Smith, S. Harput, P.L. Coletta, S. Evans, S. Freear, Increasing the sonoporation efficiency of targeted polydisperse microbubble populations using chirp excitation, IEEE Trans. Ultrason., Ferroelectr. Freq. Control 60 (2013) 2511–2520.

[12] M.J.K. Blomley, J.C. Cooke, E.C. Unger, M.J. Monaghan, D.O. Cosgrove, Microbubble contrast agents: a new era in ultrasound, Br. Med. J. 322 (2001) 1222–1225.

[13] I.W. Stewart, The Static and Dynamic Continuum Theory of Liquid Crystals, Taylor & Francis, London, 2004.

[14] A.A. Doinikov, A. Bouakaz, Theoretical investigation of shear stress generated by a contrast microbubble on the cell membrane as a mechanism for sonoporation, J. Acoust. Soc. Am. 128 (2010) 11–19.

[15] E. VanBavel, Effects of shear stress on endothelial cells: possible relevance for ultrasound applications, Prog. Biophys. Mol. Biol. 93 (2007) 374–383.

[16] W.L. Nyborg, Acoustic streaming near a boundary, J. Acoust. Soc. Am. 30 (1958) 329–339.

[17] A. Rooney, Shear as a mechanism for sonically induced biological effects, J. Acoust. Soc. Am. 52 (1972) 1718–1724.

[18] P.A. Lewin, L. Bjørnø, Acoustically induced shear stresses in the vicinity of microbubbles in tissue, J. Acoust. Soc. Am. 71 (1982) 728–734.

[19] R. Glaser, Biophysics, Springer-Verlag, Berlin, 2001.

[20] J.S. Allen, D.E. Kruse, P.A. Dayton, K.W. Ferrara, Effect of coupled oscillations on microbubble behaviour, J. Acoust. Soc. Am. 114 (2003) 1678–1690.

[21] A. Harkin, T.J. Kaper, A. Nadim, Coupled pulsation and translation of two gas bubbles in a liquid, J. Fluid Mech. 445 (2001) 377–411.

[22] A.A. Doinikov, Translational motion of two interacting bubbles in a strong acoustic field, Phys. Rev. E (2001) 64.

[23] J. Cowley, Theoretical modelling of the collapse of a shelled Ultrasound Contrast Agent used in the treatment of cancer, 2017. http://digitool.lib.strath.ac.uk/R/?func=dbin-jump-full&object_id=28409.

[24] C.C. Church, The effects of an elastic solid surface layer on the radial pulsations of gas bubbles, J. Acoust. Soc. Am. 97 (1995) 1510–1521.

[25] P. Marmottant, S. Van der Meer, M. Emmer, M. Versluis, N. de Jong, S. Hilgenfeldt, D. Lohse, A model for large amplitude oscillations of coated bubbles accounting for buckling and rupture, J. Acoust. Soc. Am. 118 (2005) 3499–3505.

[26] A.A. Doinikov, P.A. Dayton, Maxwell rheological model for lipid-shelled ultrasound microbubble contrast agents, J. Acoust. Soc. Am. 121 (2007) 3331–3340.

[27] A.A. Doinikov, J.F. Haac, P.A. Dayton, Modeling of nonlinear viscous stress in encapsulating shells of lipid-coated contrast agent microbubbles, Ultrasonics 49 (2009) 269–275.